Geophysical Fluid Dynamics, 1974, Vol. 6, pp. 101–125

Printed in Great Britain

Rotating Hydraulics of Strait and Sill Flows†

J. A. WHITEHEAD

Woods Hole Oceanographic Institution
Woods Hole, Massachusetts 02543

A. LEETMAA‡

Department of Meteorology
Massachusetts Institute of Technology
Cambridge, Massachusetts 02139

R. A. KNOX§

Department of Meteorology
Massachusetts Institute of Technology
Cambridge, Massachusetts 02139

(*Received February 12, 1973*)

Theoretical and laboratory models of certain types of strait and sill flows are discussed. Specifically, we consider a two-layer rotating fluid; the upper layer is at rest and the lower layer flows from one large basin to another via a connecting channel. The flow is assumed to be principally in a down-channel direction. The cross-channel balance is therefore geostrophic and the Bernoulli and potential vorticity equations are simplified. We further invoke the usual non-rotating hydraulic principle of maximum transport in flow over a weir—here the end of the channel—and thereby calculate relations between transport, rotation rate, and upstream interface height. One of these relations is tested experimentally with favorable results. A nonsteady decaying flow in the same system is analyzed similarly and also compares well with experiment, as does a flow in both layers driven by an initial density imbalance. Some connections with oceanic strait and sill flows are discussed.

1. Introduction

In texts on oceanography (e.g., Sverdrup, Johnson, and Fleming (1942), ch. 15) one finds discussions of the circulations in straits connecting oceans with

†Contribution No. 3038 of the Woods Hole Oceanographic Institution
‡Present affiliation: NOAA-AOML, Rickenbacker Causeway, Miami, Florida 33149
§Present affiliation: Scripps Institute of Oceanography, La Jolla, California 92037

their Mediterranean basins. The case of the Atlantic, the Mediterranean Sea, and the Straits of Gibraltar has received perhaps the most attention. Such discussions usually focus on consequences of continuity requirements, evaporation-precipitation balances and the like to arrive at "budget" calculations of transports and exchanges. Little work appears to have been done on the dynamics of the flow and particularly on the effects of the strait itself, which typically presents a severe constriction, at least geometrically. The work which has been done to date confines itself mostly to flow in straits where friction dominates (Defant (1961), ch. 16). Although there are passages connecting basins which are long and narrow enough for friction to generate appreciable resistance to the fluid flow, most straits are short and wide enough for flows to be dominated by frictionless hydraulic principles.

At the present time, there exists a considerable body of theory and empirical knowledge in the field of hydraulics concerning the dynamics of non-rotating, frictionless flow past constrictions such as dams, weirs, and channels. A good text on such matters is Rouse (1961). One basic result which emerges is that such constrictions can act as "controls" on the flow without the agency of friction. In the case of flow over a dam, the height of water over the dam is found to "control" (i.e., to be sufficient information to calculate), the height of water in the upstream basin as well as the velocity and transport of water over the dam. This is so because only one flow of the possible flows consistent with the steady momentum equations is actually observed, and this flow can be calculated from a simple rule: that the speed of outflow is just the shallow-water wave speed based on the water height above the dam. Thus the dam "controls" the flow by blocking changes in downstream level from propagating upstream as waves. Several equivalent rules can be formulated.

In this paper we seek to apply some of these ideas to flow past a constriction in a rotating system. We shall deal with a fluid of two layers with nearly equal densities, since the "reduced gravity" allows internal rotational effects to be appreciable on a much smaller scale than would be the case for a single layer. This facilitates the construction of the laboratory experiments; it also affords a crude approximation to the continuous stratification of the oceans. We examine first a steady flow in the lower layer which transfers fluid from one large basin to another via a connecting constriction in the form of a small shallow channel. This flow is maintained by pumping fluid back into the upstream lower layer without materially altering its nearly stagnant character. Our method is to augment Bernoulli's principle with the simplest possible rotational dynamics: geostrophic balance in the cross-channel direction and conservation of potential vorticity in the flow. We retain the selection rule of hydraulics, in the form of a maximization of the transport, in order to determine the solution. Relations between transport, upstream interface

height and rotation rate are then derived, and the law connecting the latter two quantities is tested by experiment, with encouraging results. The parameters of the problem combine in such a way as to show that rotation is important when the channel width is comparable to the internal Rossby radius of deformation calculated using the density contrast and the upstream depth of the lower layer above the channel floor. We treat similarly the same flow system when it is allowed to decay in time, by turning off the pump, again with favorable experimental comparisons. A third comparison is made on a two-layer flow. This flow is produced by first blocking off the channel, filling the basins with fluids of slightly different densities, and then removing the barrier.

Our aim is not to produce detailed models of particular oceanic situations. We do apply the theoretical results to a number of observed strait and sill flows, but our emphasis to date is on understanding the most elementary dynamical schemes of hydraulic rotating flows and testing in the laboratory. We hope to refine and extend such schemes in the direction of more specific oceanic models in the future.

2. Formulation

Consider the system shown in Figure 1. A region fixed in a rotating coordinate system and consisting of two large basins connected by a channel of width b is occupied by a two-layer fluid. Each layer is homogenous and inviscid, and all motions are assumed to be in hydrostatic balance. A Cartesian coordinate system is defined as shown in Figure 1; the z-axis, rotation axis, and vertical direction are parallel. For either layer the horizontal momentum equation is:

$$\frac{D\mathbf{u}}{Dt}+f\hat{k}x\mathbf{u}+\frac{1}{\rho}\nabla_h p = 0 \tag{2.1}$$

Here $\mathbf{u}$ is the horizontal velocity, ρ the density, and p the deviation of the pressure from its motionless hydrostatic value. $\hat{k}$ is a unit vector in the z direction and f is twice the angular speed of rotation. ∇_h is the horizontal gradient operator, and $D/Dt \equiv \partial/\partial t+\mathbf{u}\cdot\nabla_h$.

Because the motions are hydrostatic, and the fluid layers are homogenous, the horizontal pressure gradients depend only on the slopes of the free surface and interface. These are functions of x and y alone, and the horizontal velocity is likewise taken to be depth independent. We can thus integrate the continuity equation:

$$\nabla_h\cdot\mathbf{u}+w_z = 0 \tag{2.2}$$

from the bottom of the layer, $z = B$, to the top, $z = T$, to obtain

$$\frac{\partial h}{\partial t}+\nabla_h \cdot h\mathbf{u} = 0 \tag{2.3}$$

where $h = T-B$ and we have used the boundary condition

$$w(T)-w(B) = \frac{Dh}{Dt}$$

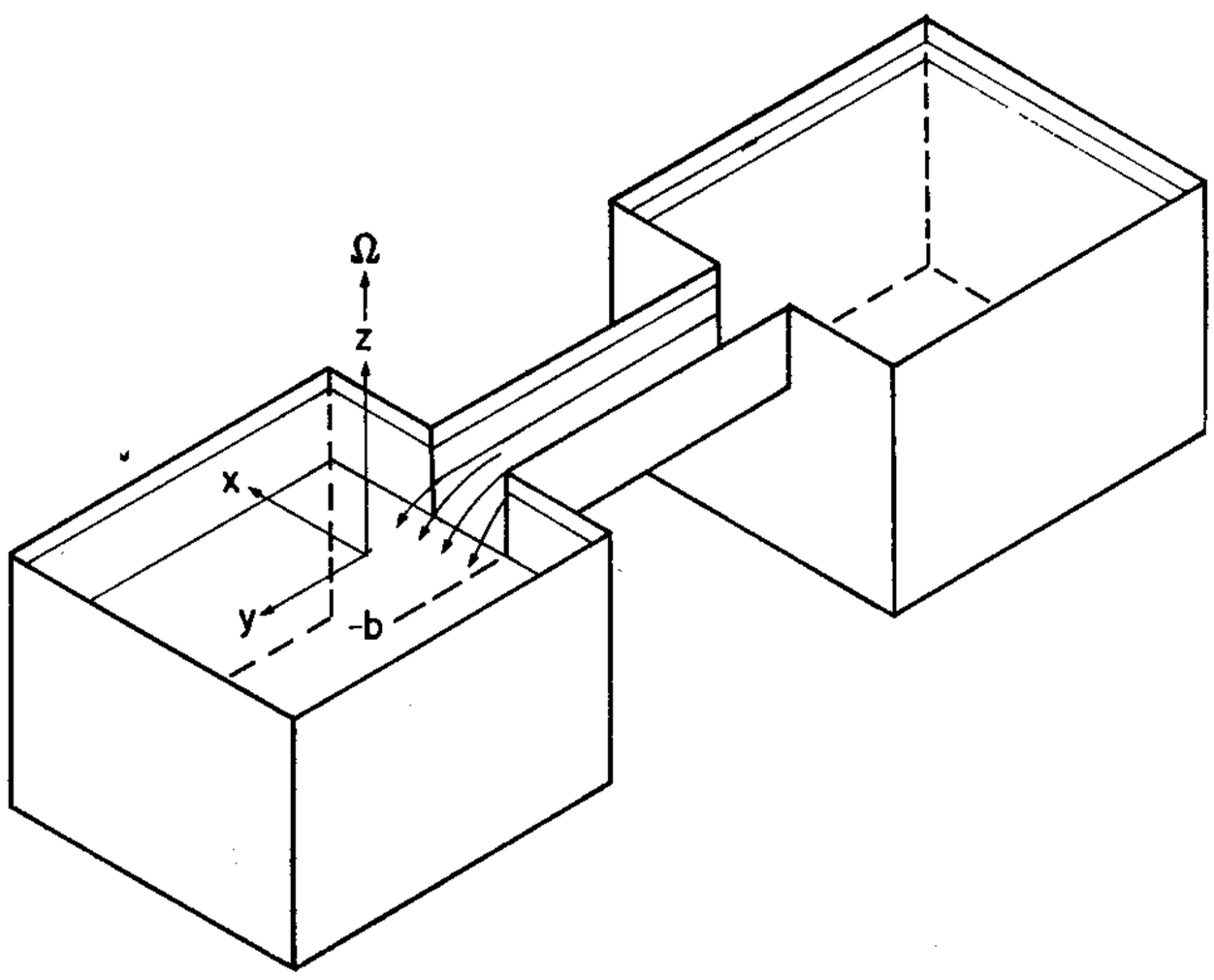

FIGURE 1 Sketch of the system studied and definition of co-ordinates.

Thus for steady motions we can define a stream function ψ:

$$\nabla x\psi\hat{k} = h\mathbf{u}. \tag{2.4}$$

Again for steady motion, scalar multiplication of the momentum Eq. (2.1) by $h\mathbf{u}$ yields Bernoulli's principle in the form:

$$J\left(\psi, \frac{1}{2}|\mathbf{u}|^2+\frac{p}{\rho}\right) = 0$$

or (2.5)

$$\frac{1}{2}|\mathbf{u}|^2+\frac{p}{\rho} = G(\psi)$$

where J is the Jacobian and G is a function of ψ alone to be determined for any particular problem.

Taking the curl of 2.1 and integrating across the layer leads to the conservation of potential vorticity:

$$\frac{D}{Dt}\left[\frac{\frac{\partial v}{\partial x}-\frac{\partial u}{\partial y}+f}{h}\right]=0$$

so that for steady motions

$$\frac{\frac{\partial v}{\partial x}-\frac{\partial u}{\partial y}+f}{h}=F(\psi) \tag{2.6}$$

where F is another function of ψ to be determined. We note, however, that (2.5) and (2.6) are not fully independent, for manipulation of the original momentum and continuity Eqs. (2.1) and (2.2) will show that $\partial G/\partial\psi = F$ [Charney (1965), acknowledging a conversation with C. G. Rossby]. Thus the choice of F and G in any particular problem must preserve this relation in order to yield a valid solution.

We further assume that the flow down the channel is straight, with little curvature of the streamlines, so that the x component of the momentum Eq. (2.1) reduces to:

$$-fv+\frac{1}{\rho}p_x=0 \tag{2.7}$$

which is the familar geostrophic relationship. Equations (2.5) and (2.6) under the same assumption respectively reduce to:

$$\frac{v^2}{2}+\frac{p}{\rho}=G(\psi) \tag{2.8}$$

$$\frac{v_x+f}{h}=F(\psi) \tag{2.9}$$

3. Steady flow in lower layer

We consider now the flow which results from steadily pumping fluid out of the lower layer of the downstream basin and into the lower layer of the upstream basin via an external circuit; the upper layer is at rest. The latter basin is sufficiently large and deep, and the pump outlet is sufficiently diffused, that

this recirculation does not alter the nearly stagnant character of the basin nor does the relatively small flux of fluid down the narrow channel. The volumes of the fluid layers are such that the interface is at a constant height h_u above the channel floor in the upstream basin, at lesser heights in the channel, and drops abruptly over the end of the channel into the downstream basin; the channel thus acts like a dam. The Bernoulli potential G is found simply by reference to the upstream basin; there the velocities are negligible and the pressure is just that due to the interface elevation, so

$$G(\psi) = \frac{p}{\rho} = \frac{\rho_2 - \rho_1}{\rho_2} g h_u = g' h_u \tag{3.1}$$

where ρ_1 and ρ_2 are the densities in the upper and lower layers, respectively. g' is often referred to as the "reduced gravity". Note that this specification of G give $dG/d\psi = 0$, so that F in the potential vorticity Eq. (2.6) must vanish to yields a consistent solution. Since in the upstream basin $F = f/(h_u + H_0)$ where H_0 is the depth below the channel floor, we must take H_0 to be very large; so $F \simeq 0$.

We now use (2.7)–(2.9) to determine the flow in the channel which results from these upstream conditions. (2.9) yields

$$\frac{\partial v}{\partial x} = -f \tag{3.2}$$

which integrates to:

$$v = -fx + v_0 \tag{3.3}$$

where v_0 is the velocity at $x = 0$. Using (2.7) and the expression for the pressure $p = gh(\rho_2 - \rho_1)$:

$$fv = g' h_x$$

where h is the interface height above the channel floor at a general location in the channel. Use of (3.3) and integration gives:

$$h = -\frac{f^2 x^2}{2g'} + \frac{f v_0 x}{g'} + h_0 \tag{3.4}$$

where h_0 is the interface height at $x = 0$.

There are two unknowns in (3.4), h_0 and v_0. The Bernoulli equation now reads:

$$\frac{1}{2} v^2 + g' h = g' h_u \tag{3.5}$$

and can be applied to the streamline at $x = 0$ to give

$$v_0 = \sqrt{2g'(h_u - h_0)} \tag{3.6}$$

We seek another relation to determine either h_u or h_0. As mentioned in the introduction, hydraulics theory uses an empirical rule for this purpose. For a discussion, see Rouse (1961), pp. 301–326. A number of such rules exist, each one leading to the correct result. It is not clear that all the rules are equivalent in the rotating situation, but we cannot resolve this uniqueness question either theoretically or experimentally within the scope of this paper. Instead, we assume the validity of the most convenient rule, that the transport of fluid Q' is maximized for a given h_u:

$$\left.\frac{\partial Q'}{\partial h_0}\right|_{h_u} = 0$$

This can be made plausible as follows: Suppose the pump is switched on to start the flow. Then the upstream level rises and fluid begins to flow down the channel at an increasing rate Q'; these are related by continuity:

$$A\frac{dh_u}{dt} = Q - Q'$$

where Q is the rate of pumping, assumed steady, and A is the basin area. At any instant of time there are several values of Q' and associated values of h_0 possible from *steady* theory; it is reasonable that when the maximum possible value of Q' becomes as large as Q, the flow reaches and maintains steady state. In appendix 1 we show that maximizing Q' is equivalent to a stability criterion of Stern (1972).

We calculate Q' for the steady state by evaluating

$$Q' = \int_{-x_b}^{0} vhdx = \int_{-x_b}^{0} \frac{g'h}{f}\frac{\partial h}{\partial x}dx = \frac{g'}{2f}[h_0^2 - h^2(-x_b)] \tag{3.7}$$

where $-x_b$ is the point at which the interface intersects either the bottom or side of the channel; in the latter case $x_b = b$. We first treat the simple case in which the intersection is on the bottom. Then $h(-x_b) = 0$ and

$$Q' = \frac{g'h_0^2}{2f}$$

h_0 can be at most equal to h_u, from (3.6) so the maximum transport Q'_m is

$$Q'_m = \frac{g'h_u^2}{2f} \tag{3.8}$$

From (3.6)

$$v_0 = 0 \tag{3.9}$$

and thus from (3.3) and (3.4)

$$v = -fx \tag{3.10}$$

$$h = -\frac{f^2x^2}{2g'} + h_u \tag{3.11}$$

The value of x_b is

$$x_b = (2g'h_u/f^2)^{1/2} \tag{3.12}$$

which will be recognized, apart from the factor of $2^{1/2}$, as the internal Rossby radius of deformation based on the upstream height.

If the parameters are such that $(2g'h_u/f^2)^{1/2} \geq b$, we have a second regime. The transport calculation is now, using (3.7):

$$Q' = \frac{g'}{2f}[h_0^2 - h^2(-b)],$$

and using (3.4) we find:

$$Q' = \frac{g'}{2f}\left[\frac{f^2b^2}{2g'} + \frac{fbv_0}{g'}\right]\left[2h_0 - \frac{f^2b^2}{2g'} - \frac{fbv_0}{g'}\right].$$

It is convenient to eliminate h_0 using (3.6) to obtain:

$$Q' = \frac{1}{2}\left[\frac{fb^2}{2} + v_0b\right]\left[2h_u - \frac{v_0^2}{g'} - \frac{f^2b^2}{2g'} - \frac{fbv_0}{g'}\right]. \tag{3.13}$$

We maximize Q' with respect to v_0, which is equivalent to maximizing with respect to h_0 at fixed h_u, by (3.6). The value of v_0 at which the maximum occurs is:

$$v_{0m} = -\frac{fb}{2} + \left(\frac{2}{3}g'h_u - \frac{1}{12}f^2b^2\right)^{1/2} \tag{3.14}$$

and the value of Q' is

$$Q'_m = \left(\frac{2}{3}\right)^{3/2} bg'^{\frac{1}{2}}\left[h_u - \frac{f^2b^2}{8g'}\right]^{3/2} \tag{3.15}$$

From (3.3) and (3.14) the velocity profile is:

$$v_m = -f\left(x+\frac{b}{2}\right)+\left(\frac{2}{3}g'h_u-\frac{1}{12}f^2b^2\right)^{1/2} \tag{3.16}$$

and from (3.4), (3.6), and (3.14) the height profile is

$$h = -\frac{f^2x^2}{2g'}+\left(\frac{2}{3}g'h_u-\frac{1}{12}f^2b^2\right)^{1/2}\frac{f}{g'}\left(x+\frac{b}{2}\right)-\frac{f^2b}{2g'}\left(x+\frac{b}{6}\right)+\frac{2}{3}h_u, \tag{3.17}$$

and h_0 is

$$h_0 = \frac{2}{3}h_u+\frac{fb}{2g'}\left[\frac{2}{3}g'h_u-\frac{1}{12}f^2b^2\right]^{1/2}-\frac{f^2b^2}{12g'}. \tag{3.18}$$

Figure 2a shows the interface height, and velocity across the channel as a function of rotation, corresponding to solutions 3.10, 3.11, 3.16 and 3.17. At zero rotation the results reduce to the hydraulic results for flow over a weir:

$$\left.\begin{aligned} h &= \frac{2}{3}h_u \\ v &= v_{0m} = \left(\frac{2}{3}g'h_u\right)^{1/2} \\ Q'_m &= \left(\frac{2}{3}h_u\right)^{3/2}b'g^{1/2} \end{aligned}\right] \tag{3.19}$$

As f increases, the fluid at $x = 0$ increases its depth and decreases its speed. The interface slopes in the cross-channel direction; the fluid at $x = -b$ decreases in depth and increases in speed. When the Rossby radius (3.12) equals b, the interface lies in the corner of the channel and the height at $x = 0$ is equal to the upstream height h_u. For faster rotation, the interface intersects the bottom of the channel.

Equations (3.8–3.18) describe how the mass flux Q'_m, the upstream height h_u, and the rotation parameter f are interrelated. These dependencies are plotted by pairs in Figure 2b; certain normalizations have been applied as explained in the captions. In particular, the transition from the slowly to the rapidly rotating regime occurs at a value of one on the abscissae. The upper curve shows h_u as a function of dimensionless rotation, δ, given a value of Q'_m, together with the height on the deep (short dashes), and shallow (long dashes) sides of the channel. h_u increases as δ^2 for slow rotation, and as $\delta^{1/2}$ for rapid rotation. The height on the deep side increases linearly with δ, until it becomes equal to h_u at transition. The center panel shows mass flux as a

function of dimensionless rotation for given upstream height. The flux is proportional to f^{-2} for slow rotation, and to $f^{-1/2}$ for rapid rotation. The lower panel shows mass flux as a function of upstream height, h_u. The flux is proportional to $h_u{}^2$ for small h_u, and it is proportional to $(h_u - \text{a constant})^{3/2}$ for larger h_u.

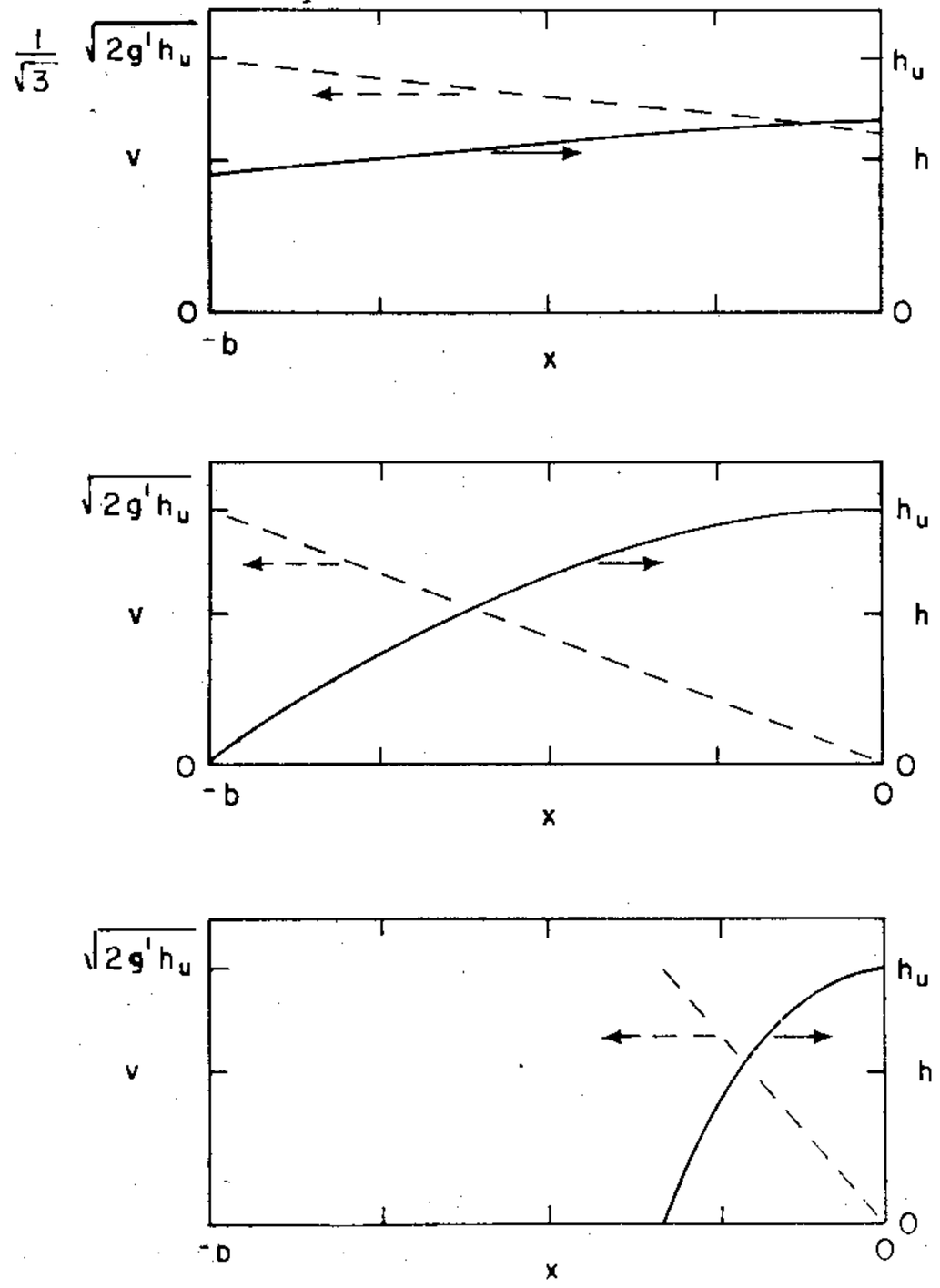

FIGURE 2a Theoretical predictions of velocity, and height of fluid in the channel for slow rotation (top), at transition (middle), and for rapid rotation (bottom).

4. Steady flow: laboratory experiment

In order to test the results of the previous section a laboratory experiment was conducted in the Hydrodynamics Laboratory of the Woods Hole Oceanographic Institution. The apparatus, shown schematically in Figure 3, consisted of a cylindrical plexiglas container 28 cm in diameter. This was divided in half by a vertical 1/4-inch plexiglas wall. Into a rectangular notch in the wall was cemented a channel 3.1 cm wide by 6 cm long by 15 cm deep; the channel floor was 45 cm above the tank bottom. A submersible pump in the bottom of one section fed the bottom of the other section via a tube, the outlet of which was in the middle of a bed of crushed rock. The entire tank was

mounted on a variable-speed rotating turntable. The pump was tested to ensure that its pumping rate was unaffected by rotation.

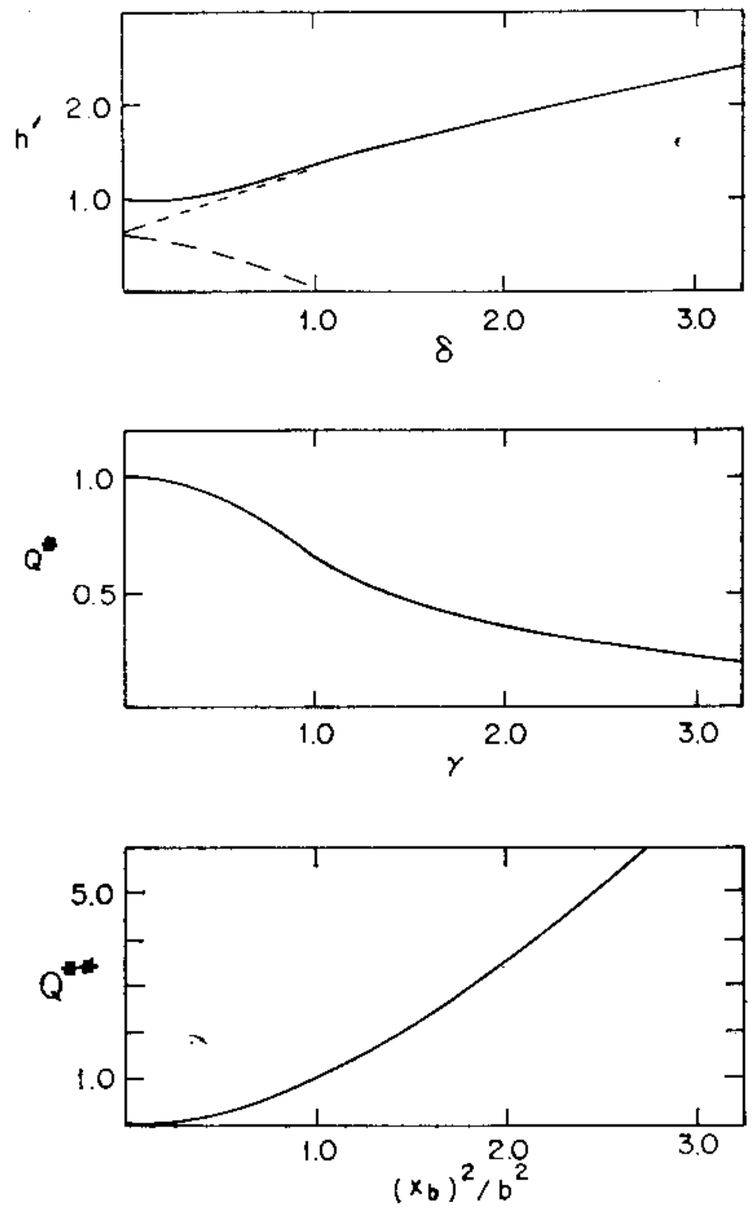

FIGURE 2b Top, theoretical prediction of nondimensionalized and normalized upstream height (Eqns. 3.8 and 3.15) $h' = h_u(\delta)/h_u(0)$ as a function of the rotation parameter $\delta = [3f^2b^2/8g'h_u(0)]^{1/2}$. Middle panel, theoretical predictions of nondimensionalized and normalized transport $Q^* = Q'_m(\gamma)/Q'_m(0)$ as a function of a rotation parameter defined as $\gamma = fb/(2g'h_u)^{1/2}$. Bottom panel, theoretical predictions of nondimensionalized and normalized transport $Q^{**} = 8g'Q_m/f^3b^4$, as a function of upstream height $4x_b^2/b^2 = 8g'h_u/f^2b^2$.

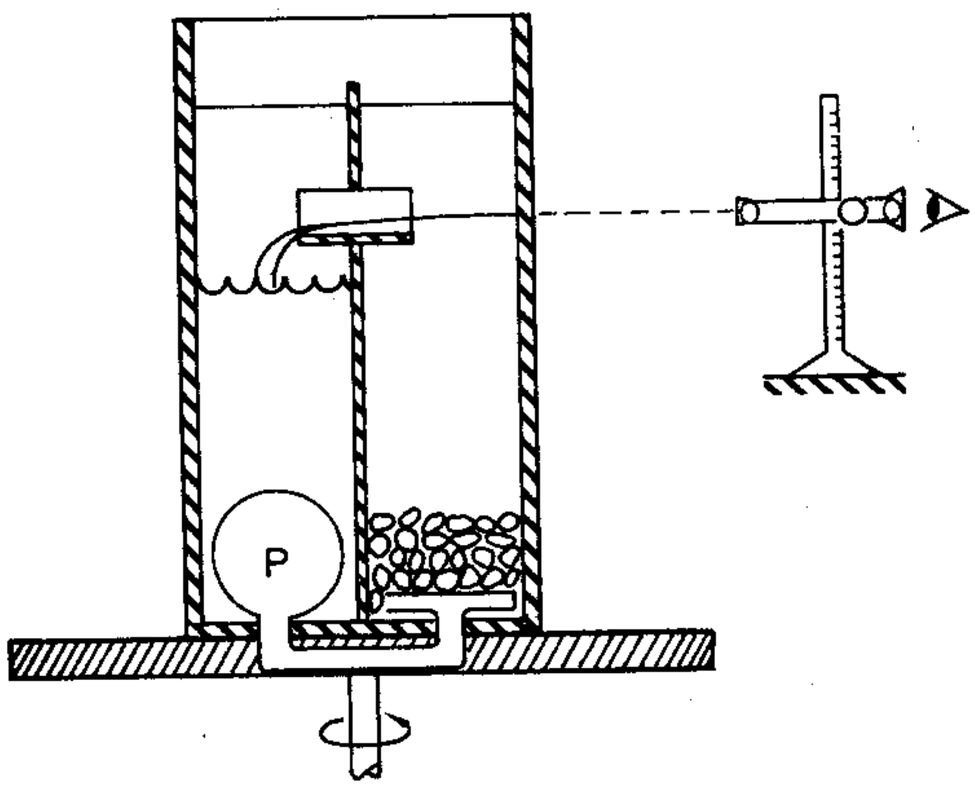

FIGURE 3 Schematic of the experimental apparatus.

Both halves of the tank were filled to the channel floor with an alcohol-water mixture with specific gravity 0.855 at 20°C and 0.838 at 40°C. The upper layer was kerosene of specific gravity 0.805 at 20°C and 0.786 at 40°C so that values of g' were 57.3 cm/sec^{-2} at 20°C and 60.8 cm/sec^{-2} at 40°C. Upstream height was measured in two ways. For low rotation rates, a depth micrometer connected to an ohmmeter was driven downward by a small motor until contact with the lower layer caused the ohmmeter to jump. The drive was then stopped and the micrometer was read. For larger rotation rates, a cathetometer was used to sight the outer edge of the upstream interface. The necessary corrections for purely centrifugal distortion of the interface were made.

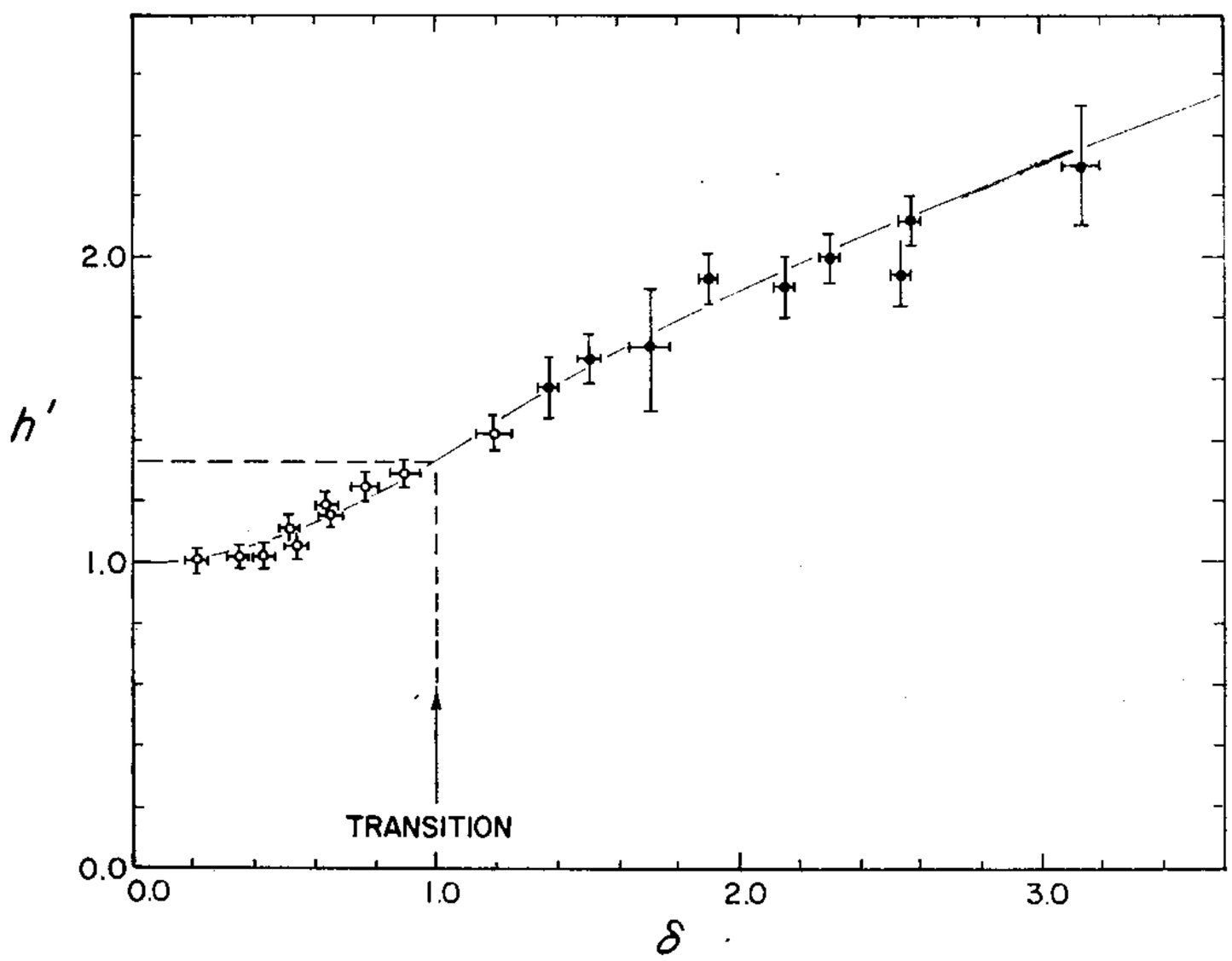

FIGURE 4 Comparison of observations with predictions for steady flow in the lower layer (Eqns. 3.8 and 3.15), $h' \equiv h_u(\delta)/h_u(0)$, $\delta \equiv [3b^2f^2/8g'h_u(0)]^{1/2}$.

The experiment began by turning on the pump without rotation, allowing the flow to become steady, and measuring h_u. Then the apparatus was spun up to a selected rotation rate; after the flow again became steady, the new value of h_u was measured. Data of this type for a range of rotation rates and for different pumping rates are shown in Figure 4; as explained in the caption, the normalization places data for all pumping rates on the same curve. It is evident that the data fall on the theoretical curve within the error estimates of the experiments.

Pictures of the flow through the channel opening are shown in Figure 5. Some of the predicted features are evident in the pictures. The cross-stream

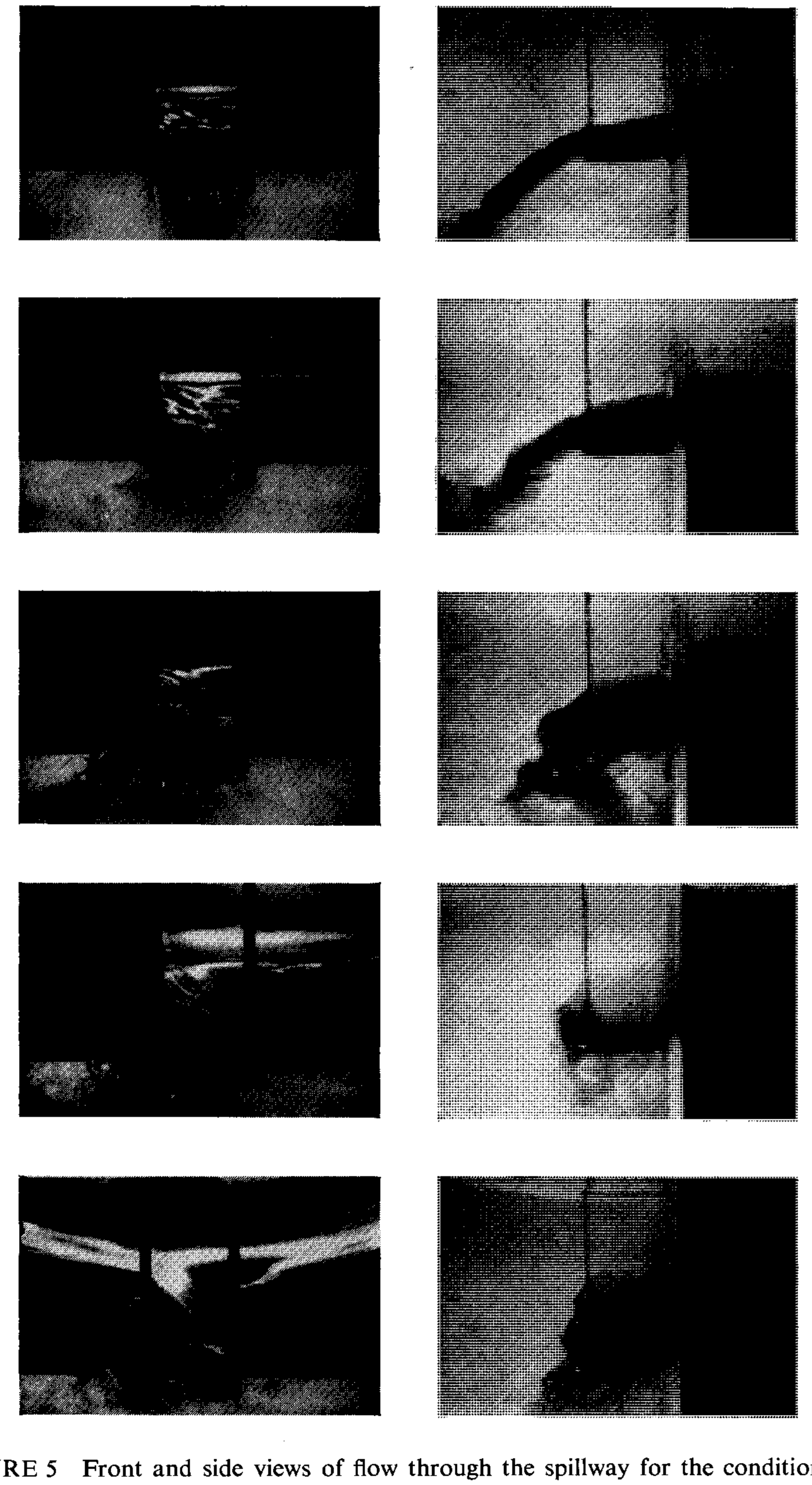

FIGURE 5 Front and side views of flow through the spillway for the conditions $\delta =$ 0.0, 0.497, 0.927, 1.30, and 2.01, respectively, from top to bottom. Although these pictures show a considerable amount of surface waves and ripples in the channel, the true steady flow was considerably smoother than these pictures indicate. The waves are shown here because they afford the viewer a clearer picture of the position of the interface.

tilt of the interface is clearly evident, and it is seen to increase with increasing rotation. The downstream tilt of the interface along the deep side of the flow is seen to decrease with increasing rotation, i.e., h_0 approaches h_u. There are other features not encompassed by the theory, however. Waves and ripples are seen; these are probably formed by the abrupt channel entrance, or are the result of the small flows in the upstream basin. Also, at high rotations the interface does not intersect the channel floor, even though the parameters are such that it should do so. One possible reason is frictional effects. The inviscid theory presented above yields zero height and the largest velocity at this intersection, and one may expect this singular situation to be frictionally modified in a real flow.

5. Transient flow of lower layer

To learn whether the steady dynamics developed in section 3 might have a greater range of validity, experiments were performed just as described in section 4 except that once the flow had become steady, the pump was switched off. Measurements of h_u as a function of time were then taken and compared with a simple quasi-steady theory. This theory is obtained by supposing that the time rate of change of h_u required by continuity is proportional to the flux down the channel as computed by steady theory, or:

$$A\frac{dh_u}{dt} = -\frac{h_u^2 g'}{2f} \text{ if } \frac{f^2b^2}{2g'} > h_u \tag{5.1}$$

and

$$A\frac{dh_u}{dt} = -\left(\frac{2}{3}\right)^{3/2} bg'^{1/2}\left(h_u - \frac{1}{8}\frac{f^2b^2}{g'}\right)^{3/2} \text{ if } \frac{f^2b^2}{2g'} < h_u \tag{5.2}$$

where A is the area of the basin. (5.1) integrates to give

$$h_u = \frac{2fA}{g'(t+t_0)} \text{ if } \frac{f^2b^2}{2g'} > h_u \tag{5.3}$$

while (5.2) gives:

$$h_u = \frac{f^2b^2}{8g'} + \frac{27A^2}{2g'b^2(t+t_1)^2} \text{ if } \frac{f^2b^2}{2g'} < h_u \tag{5.4}$$

where t_0 and t_1 are integration constants allowing h_u to assume given initial values and to have the correct value at the transition between regimes. Note that the form of the time dependence of h_u changes at transition from a -2 power law to a -1 power law.

Figure 6 shows three experimentally determined curves of h_u vs. t for three different rotation rates, and it is seen that all three sets of data follow the -1 power law quite closely. (Data could not be taken soon enough after the stopping of the pump to obtain points in the -2 power law range).

6. Flow in two directions

Another set of laboratory experiments was performed to simulate flow in both directions driven by a salinity imbalance as occurs, for instance, through the Straits of Gibraltar connecting the Mediterranean Sea with the Atlantic Ocean. The basin was 29 cm in diameter and 30 cm deep. A barrier was

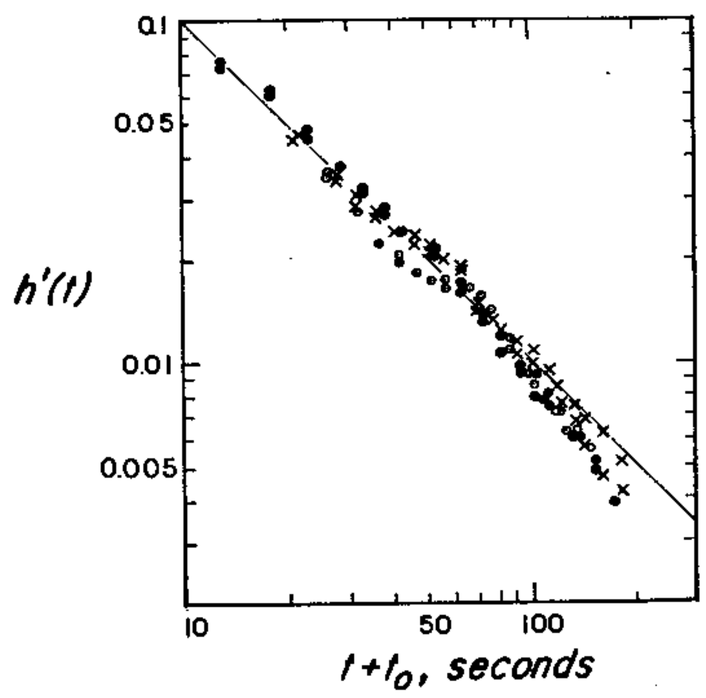

FIGURE 6 Observations of the emptying of a basin. For the data labeled ⊙, X, and ● the rotation rate is 1.1, 0.83, and 0.38 revolutions per second, respectively; $h'(t)$ is defined as $g'h_u'(t)/2fA$, and t_0 is defined as $2fA/g'h_u(0)$. The line is equation (5.3).

cemented across the diameter of the tank with an opening 3 cm wide. A sliding door with water-tight edges was fitted to the opening so that the two reservoirs on each side of the barrier could be isolated. A handle was attached to the door so that the door could be raised when the container was rotating. The procedure was to fill up the tank with 4 cm of salt water which had a density ρ equal to $1.0182 \pm .00005$, to close the gate, and then to add enough salt to one side to make density on that side $1.0280 \pm .00005$. After both reservoirs were thoroughly mixed, the container was spun up on the turntable; the gate was raised for a specified period of time, t, then lowered again; the turntable was stopped; liquids on both sides were thoroughly stirred; and density of the two samples was determined using a precision hydrometer. If $|\Delta\rho|$ denotes the difference between the initial and final density of one

reservoir and if $\rho_2-\rho_1$ denotes the initial density difference between the reservoirs, then the flux Q out of a reservoir in time t is just

$$Q=\frac{|\Delta\rho|V}{t(\rho_2-\rho_1)},$$

where V is the reservoir volume. Such a measure of flux is plotted as a function of rotation rate in Figure 7.

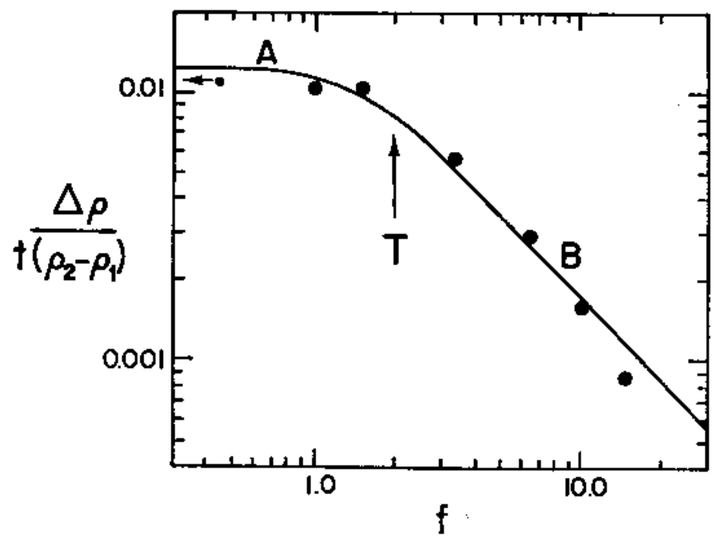

FIGURE 7 Experimental measurements for a double flow system compared with equation (6.9) (curve "A" which is valid up to the transition point labelled "T"), and equation (6.10) (curve "B", valid at values of f greater than T).

The methods of section 3 provide a simple way to calculate the flux Q as follows: Let subscript 2 refer to the heavy lower fluid and subscript 1 to the light upper fluid, and let H be the total depth of fluid above the opening. Then

$$h_1+h_2=H.$$

In place of (3.3) we now have

$$v_1=-fx+c_1 \tag{6.1}$$

$$v_2=-fx+c_2 \tag{6.2}$$

where the center of the gap is at $x=0$. Since both layers move, the condition of geostrophic balance now involves the velocity change across the interface:

$$f(v_2-v_1)=\frac{g'\partial h_2}{\partial x}. \tag{6.3}$$

Combining (6.1)–(6.3) we obtain

$$h_2=\frac{f(c_2-c_1)}{g'}x+D. \tag{6.4}$$

Mass continuity requires that:

$$\int_{-L}^{L}(v_2h_2+v_1h_1)dx = 0 \quad (v_2 > 0, v_1 < 0)$$

where the channel walls are at $x = \pm L$, and this leads to:

$$D = -\frac{Hc_1}{c_2-c_1}.$$

A relation between c_2 and c_1 is now obtained from energy considerations. The fluid along the walls $x = \pm L$ moves two-dimensionally, and for these thin layers we may equate the gain of kinetic energy in a time Δt to the release of potential energy due to change in the density field as the two fluids advance in opposite direction. An analogous calculation is performed by Yih (1965, p. 136) for the non-rotating case. One finds eventually

$$\frac{\rho_1 v_1^2}{h_2}+\frac{\rho_2 v_2^2}{h_1} = g(\rho_2-\rho_1)$$

or approximately

$$\frac{v_1^2}{h_2}+\frac{v_2^2}{h_1} = g'$$

where v_1, h_1, v_2, h_2 are to be evaluated at $x = \pm L$. Using $v_1h_1+v_2h_2 = 0$ and $h_1+h_2 = H$, we obtain

$$v_2 = \sqrt{\frac{g'}{H}(H-h_2)^2}$$

and evaluating this expression at $x = \pm L$ gives

$$c_2-c_1 = \sqrt{g'H},$$

which is the relation sought. We now evaluate the mass flux in, say, the lower layer

$$Q = \int_{-L}^{L} v_2h_2\,dx$$

using 6.2, 6.3, and the relations between c_1, c_2, and D. After some algebra we obtain

$$Q = A_1+A_2c_2(c_2-\sqrt{g'H})$$

where A_1 and A_2 are constants. Maximizing Q with respect to the last remaining free parameter c_2 then gives

$$c_2 = \frac{1}{2}\sqrt{g'H}$$

This is the same result obtained by Yih (1965) for the nonrotating case. The situation is seen to be symmetric in that the interface lies at depth $H/2$ in midchannel:

$$h_2 = f\sqrt{\frac{H}{g'}}x + \frac{H}{2}$$

and the velocities are equal and opposite there:

$$c_2 = -c_1 = \frac{1}{2}\sqrt{g'H.}$$

We rewrite these results as:

$$h_2 = \frac{H}{2}\left[1 + \frac{x}{x_0}\right] \tag{6.5}$$

$$x_0 = \frac{1}{2}\sqrt{\frac{g'H}{f^2}} \tag{6.6}$$

$$v_2 = \frac{1}{2}\sqrt{g'H}\left[1 - \frac{x}{x_0}\right] \tag{6.7}$$

$$v_1 = -\frac{1}{2}\sqrt{g'H}\left[1 + \frac{x}{x_0}\right] \tag{6.8}$$

$$Q = \frac{1}{2}\sqrt{g'}\, H^{3/2}L\left[1 - \frac{1}{3}\frac{L^2}{x_0^2}\right] \tag{6.9}$$

If the parameters are such that $x_0 < L$, the interface intersects the surface and bottom, not the channel walls. We simply assume that the same symmetric flow geometry obtains, with stagnant regions near both walls. In this case the transport integral yields a law similar to (3.8)

$$Q = \frac{1}{6}\frac{g'H_0^2}{f}. \tag{6.10}$$

Equations (6.9) and (6.10) represent the slowly and rapidly rotating regimes, respectively. These calculations are plotted in Figure 7, and agree with the experimental observations.

7. Discussion and possible applications

In this section predictions from the previous formulae will be applied to a number of natural strait and sill flows. This is done principally to illustrate the possible application of the theories, to outline their weaknesses, and to suggest future refinements.

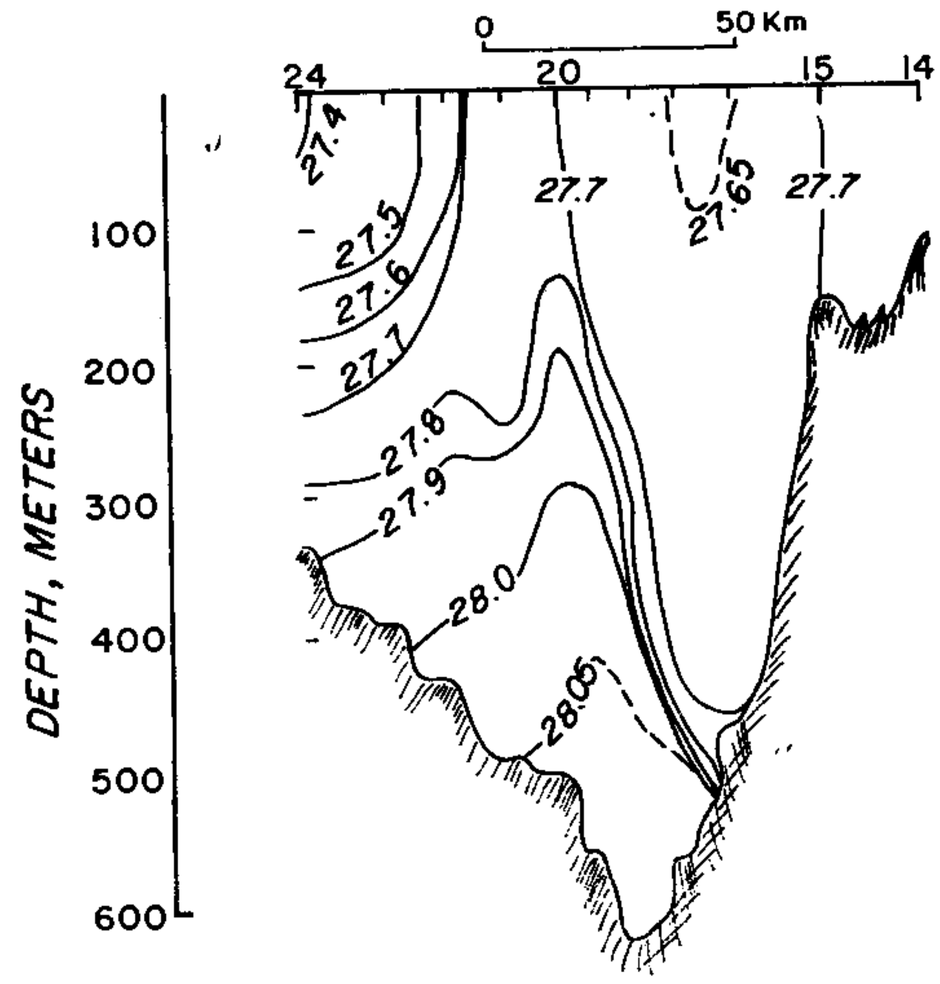

FIGURE 8 A density section in the vicinity of the shallowest part of the sill in the Denmark Straits. Data taken from Grant (1968).

We will first compare the model analyzed in section 3, with the flow of water from the Norwegian Sea spilling southward through the Denmark Straits. Such Norwegian sea water spills southward over three sills, one in the Denmark Straits, one south of Iceland, and one (the deepest sill) in the Faroe-Bank channel. Observations indicate that the greatest volume flows through the Denmark Straits, estimated at 5×10^6 m^3/sec (Worthington, 1970). A section of the density (σ_t) is shown in Figure 8 at the shallowest sill depth, the data taken from Grant (1968). The dense water spilling out of the Norwegian Sea has $\rho = 1.02805$ while the adjacent water has $\rho = 1.02770$. The sill in the Denmark Strait is approximately 620 meters below the surface of the ocean

at its shallowest point. It is difficult to estimate the upstream depth of the deep water due to the influence of the surface Greenland Current in this section. For purposes of comparison with the theoretical prediction we will take the strait to be 100 km wide, $g' = .333 \times 10^{-2}$ m/sec^2, $f = 1.338 \times 10^{-4}$ sec^{-1}, $h = 410$ m (a minimum estimate read as the minimum depth of the $\sigma_t = 27.91$ line), and $h = 620$ meters (maximum estimate assuming this water exists at the surface upstream in the Norwegian Sea as shown, for instance, in Dietrich's Atlas (1969)). In applying these numbers to flow in a rectangular channel, we must first inquire whether the strongly rotating limit Eq. 3.8 or the weakly rotating limit Eq. 3.15 is valid, which is determined by whether the Rossby deformation radius $x_b = (2g'h_u/f^2)^{1/2}$ is greater or less than the strait width, b. Using the above numbers x_b comes out to be approximately 12 km in the first case, and 15 km in the second, which is considerably less than b, so Eq. 3.8

$$Q' = \frac{g'h^2}{2f}$$

is appropriate, and yields lower and upper estimates of 2.1×10^6 and 4.8×10^6 m^3/sec. Both are well within an order of magnitude of the measured values, and the latter is within ten percent. One can also estimate the interface slope as h_u/x_b which is 34 m/km for the theoretical estimate, using the smaller value of h_u and 41 m/km for the theoretical estimate using the larger value of h_u. The sharp density jump from $\sigma_t = 27.7$ to $\sigma_t = 27.9$ or above in Figure 8 has a slope of approximately 25 m/km and so the theoretical estimates are larger by forty to eighty percent.

The above numbers indicate that the correspondence between theory and observation is reasonably good. However, we must point out a number of pitfalls:

1) The formula 3.8 can be derived by a simple consideration of geostrophic balances, and most mass flux measurements are obtained by taking this into account in some way.

2) The geometric details of the flow field may possess many irregularities which differ from the simple, stationary pattern described by theory.

3) There are many indications that the flow through the Denmark Straits is sporadic in nature and it perhaps even shuts off at times, which would indicate that at times the flow differs considerably from the stationary model described here.

Before comparing the predictions with a second natural sill flow, it is interesting to calculate a "drainage time" for the Norwegian Sea basin using the predictions of section 5, in particular Eq. 5.3, which, with the constants

which we have assumed for the Denmark Straits and an area of the Norwegian Sea of 10^6 km^2, becomes

$$h_u = \frac{8\times 10^{10}}{t+t_0}$$

where, if h_u is 620 m at $t = 0$, $t_0 = 1.29\times 10^8$ sec. Thus an initial height h_u will be halved in a time $t = 1.29\times 10^8$ sec $\approx$ 4 years, which would imply that the flow through the straits would not respond greatly to the yearly cycle, but that it would remain relatively uniform even if most of the water were formed in a few winter months.

We can make a second comparison with a recent series of measurements by Metcalf and Stalcup (private communication) made in the Anegada Passage, which separates the eastern Caribbean Basin from the Guiana Basin of the Atlantic Ocean. Although these measurements are still being analyzed, the picture emerges of a 3.7°C mass of water, approximately 100 meters deep under 4°C water flowing through a passage approximately 5 km wide. The 4° isotherm continues to lie 100 meters above the sill maximum for a considerable distance upstream. Measurements from current meters yield estimates of volumetric flow of 10^5 m^3/sec. The isotherms have a small tilt of about 5 m/km. For purposes of comparison with theory of section III we take $h_u = 10^2$ m, $g' = 4\times 10^{-4}$ m/sec^2, $b = 5\times 10^3$ m, $f = .45\times 10^{-4}$ sec^{-1}. Using these numbers the Rossby radius x_b is 6.2 km, slightly greater than the 5 km opening, and we get a mean change in depth of 16 m/km, which is about three times greater than visual inspection of the Metcalf-Stalcup data appears to yield. The slowly rotating mass flux prediction Eq. 3.15 is $Q' = 4.03\times 10^4$ m^3/sec which is a little less than half the current meter estimates derived from current meter readings, which average about 20 cm/sec.

Three physical processes can account for the discrepancy between observation and theory: (1) tidal fluctuations which are apparent in all of the velocity measurements in the sill, (2) the long channel in the Anegada Passage, with a large depression immediately in front of the sill—this depression might generate unusual vortex-stretching or three-dimensional effects, (3) frictional effects generated by the long passage.

A third comparison can be made with the flow through the Straits of Gibraltar. Water in the Mediterranean is roughly two parts per thousand more saline than the Atlantic. For these purposes we take the reduced gravity caused by the differences between saline Mediterranean water and fresher North Atlantic water to be

$$2\times 10^{-2}\ \text{m/sec}^2\left(\frac{\Delta\rho}{\rho} = 0.002\right),$$

the minimum sill depth to be 286 m (Frassetto, 1960), width of the opening (2L) to be 7 km (the width of the 100-meter depth contour at the sill) and f to be 0.85×10^{-4} sec^{-1}. These numbers give a Rossby radius of deformation as defined for flow in both directions (Eq. 6.6) of $x = 14$ km, four times the half width of the strait. We thus use Eq. 6.9 and calculate $Q = 1.16 \times 10^6$ m^3/sec, which is surprisingly close to Lacombe's (1961) measurements of 1.2×10^6 m^3/sec. The slope of the interface predicted can be estimated as $2x_0/H = 10.2$ m/km. It is hard to compare this number with observations in the straits because of the great temporal and seasonal fluctuations that occur there, but it appears to agree reasonably well.

In comparing the theory of section 6 with field observations, it must be emphasized that any close numerical agreement between observations and the present theory is fortuitous. The influences of rough topography will probably always inject an uncertainty of at least a few tens of percent into the values of width and depth of the sill. Likewise, tidal, seasonal, and meteorological fluctuations will always inject temporal variations into field measurements, and such variations might not easily be incorporated into corrections to the above theory. Lastly, the energy dissipation due to turbulent circulations, unaccounted for in the theory, would certainly appear to play some dynamic role in the Straits of Gibraltar, where fluctuations are often as large as the mean flow.

In summary, a number of idealized models have been made of strait and sill flows; these have been theoretically analyzed and tested in the laboratory. A comparison with observed flows, which appear to have the various limits of the theoretical analysis, has been performed to indicate the appropriateness of these models. It is hoped that field workers will continue to test these predictions against their observations of other oceanic flows, cautioned by the fact that a meaningful comparison can only be expected with flows in the vicinity of the shallowest and narrowest sill.

Acknowledgements

The authors are happy to record their indebtedness to Professor Henry Stommel for many hours of fascinating dialogue after having originally suggested the problem. The photographs were taken with the able assistance of Robert Frazel of the Hydrodynamics Laboratory of Woods Hole Oceanographic Institution. During this period of research, the authors were supported by Office of Naval Research contract NOOO14–66–CO241 (J.A.W.), National Science Foundation grant GA–35447 (J.A.W.), National Science Foundation grant A–30729X (A.L. and R.A.K.), and Office of Naval Research contract NOOO14–67–A–0204–0048 (R.A.K.).

Appendix

Comparison with Stern's Stability Criterion. Stern (1972) has considered geo-

strophically balanced flow down a channel whose bottom slopes in the cross-channel direction, the slope chosen so that the flow has uniform thickness and velocity. He inquires as to what happens when this flow passes through a contraction (a section in which the channel walls are closer together); preserving geostrophic balance, energy (Bernoulli function), and potential vorticity. For sufficiently severe contractions, it is not possible for the flow to preserve these quantities and the given upstream mass flux; Stern terms the flow "critical" when even an infinitesimal contraction leads to no solution. (In a real flow a shock or other phenomenon outside the grasp of the theory would presumably occur.) The "critical" condition turns out to be the same as the nonrotating one, that is, that uniform upstream speed is just the shallow-water wave speed based upon the uniform upstream thickness. In a later work (personal communication), Stern has expanded this idea to include upstream flows with thickness and speed variation in the cross-stream direction. The "critical" criterion is found to be, in the notation of section 3.

$$\int_{-b}^{0}\left(\frac{1}{g'h^2}-\frac{1}{hv^2}\right)dx = 0. \tag{A 1.1}$$

In the nonrotating case the condition $v^2 = gh$ satisfies Eq. (A 1.1) identically. Note that this criterion can only apply in what we have termed the slowly rotating regime in which the fluid touches both channel walls. Mathematically, this is because, in deriving Eq. (A 1.1), Stern has used the geostrophic relation

$$dx = (g'/fv)dh \tag{A 1.2}$$

to convert from an integral over h to one over x, and in our rapidly rotating regime v vanishes at $x = 0$; the Jacobian of this transformation therefore vanishes. Physically, Stern's infinitesimal contraction has the effect of making an infinitesimal reduction in the channel cross-section available to transport mass; this infinitesimal reduction makes a flow of the specified upstream flux, Bernoulli function, and potential vorticity impossible when the upstream flow is "critical". In our rapidly rotating regime, however, a similar infinitesimal contraction only yields a *doubly* infinitesimal reduction in cross-section; the intersection at $x = -b$ of the interface with the channel floor is pushed infinitesimally toward $x = 0$, and the thickness of the moving layer is itself infinitesimal at the intersection. Phrased another way, $\partial Q'm/\partial b$ vanishes at the transition point from slowly to rapidly rotating regimes (cf. 3.15) and also, of course, throughout the rapidly rotating regime.

Restricting ourselves to the slowly rotating regime, therefore, we evaluate the integral in A 1.1 using our solutions of section 3. We first transform to an

integration over h using the geostrophic Eq. (A 1.2) and Bernoulli's Eq. 3.5, we have:

$$\frac{1}{2f(2g)^{1/2}}\int_{h(-b)}^{h_0}\frac{2h_u-3h}{h^2(h_u-h)^{3/2}}\,dh=0 \qquad \text{(A 1.3)}$$

which is more conveniently written as

$$\frac{1}{2f(2g)^{1/2}}\left[2\int_{h(-b)}^{h_0}\frac{dh}{h^2(h_u-h)^{1/2}}-\int_{h(-b)}^{h_0}\frac{dh}{h(h_u-h)^{3/2}}\right]=0$$

These can be integrated to give

$$-\frac{1}{f(2g)^{1/2}}\cdot\frac{1}{h(h_u-h)^{1/2}}\Bigg|_{h(-b)}^{h_0}=0$$

which is, in terms of velocities

$$-\frac{1}{f}\left[\frac{1}{h_0v_0}-\frac{1}{h(-b)v(-b)}\right]=0 \qquad \text{(A 1.4)}$$

or

$$-\frac{1}{f}\left[\frac{h(-b)v(-b)-h_0v_0}{h_0v_0h(-b)v(-b)}\right]=0 \qquad \text{(A 1.5)}$$

This last form shows that Stern's criterion in this problem is satisfied if the transport per unit width is the same at both channel walls. Simple substitution for h_0, v_0, $h(-b)$, $v(-b)$ from Eqs. (3.14), (3.16), (3.17), (3.18) shows that indeed $h_0v_0 = h(-b)v(-b)$ and Stern's criterion for critical flow is therefore satisfied by our solutions in section 3. Therefore, Stern's (critical) condition is equivalent to maximizing mass flux for the weakly rotating case.

References

Charney, J., "The Gulf Stream as an inertial boundary layer," *Proc. Nat. Acad. Sci.* **41,** 10, 731–740 (1955). Also found in *Wind-Driven Ocean Circulation*, A. R. Robinson, *ed.*, Blaisdell Publishing Company, New York (1963).

Defant, A., *Physical Oceanography*, Vol. I, Chapter XVI, Pergamon Press, New York (1961).

Dietrich, G., *Atlas of the Hydrography of the Northern North Atlantic Ocean*, Conseil International pour l'Exploration de la Mer, Service Hydrographique, Charlottenlund Slot, Danemark (1969).

Frassetto, R., "A preliminary survey of the thermal microstructure in the Straits of Gibraltar," *Deep-Sea Research* 7, 3, 156–162 (1960).

Grant, A. B. *Atlas of Oceanographic Sections, Davis Strait-Labrador Basin-Denmark Strait* 1965–1967, Atlantic Oceanographic Laboratory, Bedford Institute, unpublished manuscript (1968).

Lacombe, H., "Contribution à l'étude de régime de Détroit de Gibraltar," I. Etude dynamique, *Cah. Océanog.* **XIII**, 2, Fév (1961).

Rouse, H., *Fluid Mechanics for Engineers*, Dover Publishing Company, New York (1961).

Stern, Melvin E., "Hydraulically critical rotating flow," *Phys. Fluids* **15**, 2062–2064 (1972).

Sverdrup, H. U., Johnson, M. W. and Fleming, R. H., *The Oceans*, Prentice-Hall Inc., Englewood Cliffs, New Jersey (1942).

Worthington, L. V., "The Norwegian Sea as a mediterranean basin," *Deep-Sea Research* **17**, 77–84 (1970).

Yih, C. S., *Dynamics of Nonhomogenous Fluids*, MacMillan Company, New York (1965).